Wind Driven Optimization based Optimal Energy Management of Microgrid Impregnated with Renewable Energy Sources Article Info ABSTRACT

Article · February 2024

DOI: 10.46657/ajresd.2023.5.2.13

3 authors:

Nabil Mezhoud
Université 20 août 1955-Skikda
19 PUBLICATIONS **32** CITATIONS
SEE PROFILE

Bahri Ahmed
Université de Ghardaia
15 PUBLICATIONS **17** CITATIONS
SEE PROFILE

Bilel Ayachi
Université 20 août 1955-Skikda
11 PUBLICATIONS **10** CITATIONS
SEE PROFILE

Wind Driven Optimization based Optimal Energy Management of Microgrid Impregnated with Renewable Energy Sources

Nabil Mezhoud[1], Ahmed Bahri[2], Bilel Ayachi[1]

[1]Electrical Engineering Department, Faculty of Technology, LES Laboratory, University 20 Août 1955-Skikda, Skikda 21000, Algeria
[2]Department of Automatics and Electromechanics, Faculty of science and technology, MESTE Laboratory, Ghardaïa University, Ghardaïa, 47000, Algeria
*Corresponding author; Email: n.mezhoud@univ-skikda.dz

Article Info

Article history:

Received, 16/11/2023
Revised, 30/11/2023
Accepted , 05/12/2023

Keywords:

Distributed generator
Energy storage
Micro-grids
Optimal energy management,
Renewable energy sources
Wind driven optimization

ABSTRACT

The desire for increased dependability, high energy quality, reduced cost, and a clean environment has led to a rise in the use of renewable energy sources (RES) in recent years, such as solar energy and wind energy. In this study, the optimal energy management (OEM) problem of a microgrid (MG) infused with RES is solved through the application of a nature-inspired meta-heuristic approach termed Wind Driven Optimisation (WDO), which is based on atmospheric motion. Our primary purpose is to minimise the nonlinear objective function of an electrical microgrid, which is expressed by minimising the MG operating cost while accounting for various operational limits related to equality and inequality through the best possible OEM control variable adjustment. A variety of DGs, including fuel cells (FC), wind turbines (WT), photovoltaic systems (PV), micro turbines (MT), and loads with energy storage systems (ESS), have been studied and tested using the WDO approach on MG linked. The outcomes show how the suggested strategy may effectively and robustly tackle OEM problems in various operational circumstances, which is encouraging. The suggested method's outcomes were verified and compared to those of reputable references that were recently published.

I. Introduction

In recent times, there has been a notable surge in the advancement and utilisation of renewable energy sources [1]. A unique position is held by wind turbines among various energy sources. Indeed, wind energy is predicted to grow rapidly in many areas, but it can also have a substantial impact on the voltage and current quality in the network where it is injected because of its highly variable nature caused by large variations in wind speed (WS) [2].

Distributed generation (DG) has grown steadily during the last 20 years. Geographical and meteorological factors influence how DGs are integrated with renewable energy sources (RES), such as photovoltaic systems (PV) and wind turbines (WTs). Moreover, the characteristics of their output powers are unpredictable and change over time [3]. However, non-renewable energy distributed generation (DG) equipment, like fuel cells, diesel electric generators (DEG), micro gas turbines (MT), and energy storage systems, can be linked to any point in the distribution network and produce power that is predictable [3]–[4].

In a broader sense, the strategic utilization and effective management of DG units yield advantageous

outcomes in terms of power quality enhancement, minimized power losses, improved reliability, and reduced emissions. An integrated strategy that includes energy storage devices, controllable loads, and coordinated operation and control is necessary to realise the full potential of distributed generation. This opens the door for the groundbreaking paradigm known as micro-grids (MGs) to emerge [3], [5]. Basically, MGs are local distribution networks made up of several DG units, controllable loads, and energy storage devices that can function as controlled entities either connected to or apart from the main distribution grid [6]–[8]. It is crucial that the integration of DGs into MGs and their relationship with the distribution network main upstream help to optimise the general operation of the system in order to fully benefit from the operation of MGs, such as improved profitability and decreased dependence on the main network [9]–[10].

Energy management optimization is closely related concepts that aim to optimize usage in a given system. Energy management refers to the overall management of energy within a system, seeking to minimize losses and maximize energy efficiency [11].

To date, a very large number of mathematical techniques have been applied, as well as artificial smart methods, to solve the OEM problem, including:

- Evolutionary algorithms [4, 12, 13, 14 and 15].
- Swarm intelligence algorithms [11, 16, 17 and 18].
- Physical algorithms [19, 20].
- Nature inspired algorithms [21 and 22].
- Bio-inspired algorithms [23, 24, 25, 26 and 27].
- Other algorithms [28, 29, 30, 31, 32 and 33].

To handle single and multi-objective functions in electric power systems, variants of these algorithms were devised. The OEM problem has been resolved in this paper by utilising the WDO [21].

II. Problem formulation

The *OEM* is nonlinear and non-convex optimization problem with constraints. In this work, the energy management is implemented by ordering the *MG* components.

II.1. Objective function

The main goal is to minimize the operating costs of the *MG*. The general optimization problem can be presented as

$$\min\ f(x,u) = \sum_{t=1}^{nt} \cos t^t\left(x^t, u^t\right) = \min_u \sum_{t=1}^{nt}\sum_{i=1}^{ng}\left[B_{gi}\left(P_{gi}^t\right) + MP^t P_{grid}^t\right] \quad (1)$$

Subject to

$$h(x,u) = 0 \quad (2)$$

$$g(x,u) \le 0 \quad (3)$$

T is a scalar objective function, and $f(x,u)$ is the total operating cost of MG system throughout the planning horizon. The collection of nonlinear equality and inequality constraints is denoted by $h(x,u)$ and $g(x,u)$, respectively. P_{grid}^t is the active power that is bought (sold) from (to) the utility at time *t*; *nt* is the total number of time, *ng* is the total number of DGs including storage systems; P_{gi}^t is the active power output of i^{th} DG at time *t*; $B_{gi}(P_{gi}^t)$ is the bid of i^{th} DG at time *t*; and MP^t is the exchange electricity market price between the MG and utility at time *t* [34]–[36]. The state and control variables are denoted, respectively, by *x* and *u* and given as follows.

$$x^t = P_{grid}^t \quad (4)$$

$$u^t = \left[P_{g1}^t,\ P_{g2}^t, \ldots . P_{gng}^t\right] \quad (5)$$

II.2. Constraints

1) Power balance constraints (PBC)

When the active power loss in MG is disregarded, the power balance restriction is represented as follows.

$$\sum_{i=1}^{NG} P_{gi}^{t} + P_{grid}^{t} = \sum_{d=1}^{nd} P_{L_d}^{t} \tag{6}$$

nd is the total number of load levels, while P_{L_d} is the quantity of the tenth loads level.

2) Power generation capacity constraints

Each unit in MG, including the utility, has an active power output that is constrained for stable operation by the following minimum and maximum limits:

$$P_{gi-\min}^{t} \le P_{gi}^{t} \le P_{gi-\max}^{t} \tag{7}$$

$$P_{grid-\min}^{t} \le P_{grid}^{t} \le P_{grid-\max}^{t} \tag{8}$$

Where, $P_{gi-\max}^{t}$, $P_{grid-\max}^{t}$, $P_{gi-\min}^{t}$ and $P_{grid-\min}^{t}$,are, respectively, the maximum and minimum active powers of the i^{th} *DG*, and the utility at time *t* .

3) Reserve spinning constraints (RSC)

The RS is required to keep the system reliable because of fluctuations in both load and renewable energy power. To meet the reserve spinning, the inequality constraint listed below needs to be met [37]:

$$\sum_{i=1}^{NG} P_{gi-\max}^{t} + P_{grid-\max}^{t} = \sum_{d=1}^{nd} P_{L_d}^{t} + R^{t} \tag{9}$$

The reserve spinning scheduled at time *t* is known as R^{t} .

4) Energy storage limits (ESL)

For a typical battery, the following equation and limitations can be given, as there are limits to the charge and discharge rate of storage devices during each time interval t [38]:

$$W_{ess\_t} = W_{ess\_t-1} + \eta_{charge} P_{charge} \Delta t - \frac{1}{\eta_{discharge}} P_{discharge} \Delta t \quad where \quad \begin{cases} W_{ess-\min} \le W_{ess-t} \le W_{ess-\max} \\ P_{charge\_t} \le P_{charge-\max} \ \ and \ \ P_{discharge\_t} \le P_{discharge-\max} \end{cases} \tag{10}$$

where W_{ess_t} and W_{ess_t-1} represent the batterys capacity at times *t* and *t*-1, respectively. The charge (discharge) rate permitted for a specific time frame Δt is known as $P_{charge}(P_{decharge})$; The lowest and maximum limits of the energy stored in the battery are represented by $W_{ess-\min}$ and $W_{ess-\max}$; the maximum rate of charge (discharge) of the battery during each Δt interval is denoted by $P_{charge-\max}(P_{discharge-\max})$; and the battery efficiency (yield) is denoted by $\eta_{charge}(\eta_{decharge})$.

5) Calculation of active power from (to) the network

The active power from (to) the utility is taken into consideration as a dependent variable in order to apply the active power budget constraint described in (6). The following formula is used to determine the grid power value:

$$P_{grid}^{t} = \sum_{d=1}^{nd} P_{L_d}^{t} - \sum_{i=1}^{ng} P_{gi}^{t} \tag{11}$$

The obtained P_{gi}^{t} we check whether or not satisfies the constraint (8). Therefore, $P_{grid,\lim}^{t}$ is described as:

$$P_{grid-\lim}^{t}=\begin{cases}P_{grid-\max}^{t} & si\ P_{grid}^{t}>P_{grid-\max}^{t}\\ P_{grid-\lim}^{t} & si\ P_{grid-\lim}^{t}<P_{grid-\min}^{t}\\ P_{grid}^{t} & si\ P_{grid-\min}^{t}\le P_{grid}^{t}\le P_{grid-ax}^{t}\end{cases} \tag{12}$$

It should be noted that the dependent variable, or P_{gi}^{t}, should be introduced to the objective function as a quadratic penalty term, whereas the control variables are self-controlled. The following new extended objective function to be optimised is:

$$\min_{u} F_{p}=\min_{u}\sum_{t=1}^{nt}\cos t^{t}\left(x^{t},u^{t}\right)+\lambda_{p}\left(P_{grid}^{t}-P_{grid-\lim}^{t}\right)^{2} \tag{13}$$

In (13) λ_{p} represent the penalty factor.

II.3. Bids calculation of distributed generation

According to equation (14), the DG bids are seen as quadratic.

$$B_{gi}=a_{i}P_{gi}^{\ 2}+b_{i}P_{gi}+c_{i} \tag{14}$$

1) Micro-turbine and Fuel cell

The *MT* and *FC* bids in ($/h) can be computed as follows [16], [39]:

$$B_{g}=C_{fuel}\frac{P_{g}}{\eta_{g}}+C_{inv} \tag{15}$$

P_{g} is the *DG* (*MT* and *FC*) electric power output in (kW), η_{g} is the *DG* electrical efficiency, C_{fuel} is the fuel price (gas) to supply the *DG* ($/kWh), C_{inv} is the hourly rate at which DG's investment cost is reimbursed ($/h). The annual production (AP) in (kW h/kW), the DG nominal power in (kW), and the annual cost (AC) in ($/kW-year) determine C_{inv} as follows:

$$C_{inv}=AC\frac{P_{g-nom}}{AP} \tag{16}$$

$$AC=\frac{i(1+i)^{n}}{(1+i)^{n}-1}IC \tag{17}$$

Where *IC* is the DG installation cost, *n* is the amortisation period in years, and *i* is the interest rate [40]. The fuel cell efficiency, or FC efficiency for a Proton Exchange Membrane Fuel Cell, is a non-linear function of power level and is expressed as follows [41]:

$$\eta_{FC}=\frac{1}{2.964}\left[V_{0}+\sqrt{V_{0}^{2}-4\left(V_{0}V_{Pnom}-V_{Pnom}^{2}\right)\xi}\right] \tag{18}$$

Where $\xi=P_{FC}/P_{nom}$ is the power level, P_{nom} is the rated power of FC, V_{Pnom} is the potential of the chosen cell at rated power, and V_{0} is the theoretical or thermodynamic FC potential.

2) Wind turbines and Photovoltaic

Like *MT* and *FC*, the WT and PV bids take into account the AP (kW h/kW) and AC ($/kW), which are provided by (16)–(17). These PV and WT sources cannot be controlled, and the amount of each is dependent on the availability of the primary source. According to [42]–[43], the power curve of a WT is

$$P_{WT}=\begin{cases}0 & v\le v_{ci}\\ \dfrac{v^2-v_{ci}^2}{v_{nom}^2-v_{ci}^2}P_{WT-nom} & v_{ci}<v\le v_{nom}\\ P_{nom}, & v_{nom}<v\le v_{co}\\ 0 & v\ge v_{co}\end{cases} \tag{19}$$

Where, P_{WT-nom}, v_{nom}, v_{ci} and v_{co} are, respectively, the rated power, rate of wind speed, switch-in wind speed and switch-on wind speed of *WT*; P_{WT} is the output power of *WT* and v is the wind speed [44].

The *PV* output power depends on the solar irradiation and the ambient temperature of the site as well as the characteristics of the module itself. To calculate the *PV* output power, P_{PV} , the following equation can be used.

$$P_{PV}=P_{STC}\frac{I_S}{1000}\left[1+\gamma\left(T_C-25\right)\right] \tag{20}$$

Where, P_{STC} is the *PV* maximum power under STC in (W); I_S is the solar irradiation of *PV* in (W/m^2); γ is the *PV* module temperature coefficient for power in (°C^{-1}); T_C is the temperature of the *PV* cell in (C). The temperature of *PV* module based on the Nominal Operating Cell Temperature (*NOCT*) of the module. The equation of *NOCT* model is [44]-[45]:

$$T_c=T_a+\frac{I_S}{800}\left(T_{NOCT}-20\right) \tag{21}$$

Where, T_a is the ambient temperature in (°C); T_{NOCT} is the *NOCT* of module in (°C).

3) Diesel electric generators (DEG)

The DEG fuel consumption characteristic may be calculated as a quadratic function:

$$Fuel_{DEG}=a_f P_{DEG}^2+b_f P_{DEG}+c_f \tag{22}$$

Where, $Fuel_{DEG}$ is the consumption fuel in (L/h); P_{DEG} is the *DEG* output power in (KW); α_f , b_f and c_f are the coefficients of the fuel consumption characteristic. The *DEG* bids ($/h) can be computed as:

$$B_G=C_{fuel}Fuel_{DEG}+C_{inv} \tag{23}$$

Where, C_{fuel} is the diesel fuel price in ($/L). The hourly payback amount for the DEG ($/h) investment cost is called C_{inv} and is determined by (16)

4) Electric grids

The following quadratic function can be used to describe the energy market costs in ($/h) :

$$f_{gr}=a+bP_{gr}+cP_{gr}^2 \tag{24}$$

Where, f_{gr} is the electric power in (kW) and a, b and c are the coefficients of cost.

II.4. Input random variables

1) Weibull distribution

It is often the case that a *Weibull distribution* describes the probability density function (PDF) of the wind speed at a given location [37], [43], [45]:

$$f_{P_{WT}}(P_{WT}) = \frac{k}{C}\left(\frac{P_{WT}}{C}\right)^{k-1} e^{(P_{WT}/C)^k} \tag{25}$$

The cumulative density function (CDF) of *Weibull distribution* is

$$F_{P_{WT}}(P_{WT}) = 1 - e^{-(P_{WT}/C)^k} \tag{26}$$

The CDF with its inverse is used to calculate the wind speed is

$$P_{WT} = C(-\ln(r))^{1/k} \tag{27}$$

r represents the uniformly distributed random numbers across [0, 1]. The scale and shape parameters of the *Weibull distribution* are represented by the constants *C* and *k*. The wind speed average v_m and standard deviation (SD) σ are typically used to roughly determine the parameters *C* and *k* [36–37]

$$\begin{cases} k = \left(\dfrac{\sigma}{P_{WTm}}\right)^{-1.086} \\ \text{and} \quad C = \dfrac{P_{WTm}}{\Gamma(1+1/k)} \end{cases} \tag{28}$$

Where, $\Gamma(x)$ is the gamma function defined as:

$$\Gamma(x) = \int_0^{\infty} t^{x-1} e^{-t} dt \quad \text{for} \quad x > 0 \tag{29}$$

2) Normal distribution

Basically, solar irradiation (SI) has a stochastic nature. Therefore, the PDF should be adopted. One can use a normal probability density function to describe the uncertainty of SI [45].

$$f_{IS}(I_S) = \frac{1}{\sigma\sqrt{2\pi}} e^{-(I_S-\mu)^2/2\sigma^2} \tag{30}$$

The CDF for the *normal distribution* is:

$$F_{IS}(I_S) = \frac{1}{2}\left[1 + erf\left(\frac{(I_S-\mu)}{\sqrt{2\sigma}}\right)\right] \tag{31}$$

The CDF with its inverse was used to calculate the SI:

$$I_S = \mu + \sqrt{2}.\sigma.erf^{-1}(2r-1) \tag{32}$$

r is a random variable with uniform distribution in the interval [0, 1], μ denotes the IS mean value, and σ is the IS standard deviation. The error function erf and the its inverse erf^{-1} are, respectively defined as follows

$$erf(I_S) = \frac{2}{\sqrt{\pi}} \int_0^{I_S} e^{-t^2} dt \qquad \text{and} \qquad erf^{-1}(I_S) = 1 - erf(I_S) = \frac{2}{\sqrt{\pi}} \int_{I_S}^{\infty} e^{-t^2} dt \tag{33}$$

3) Probabilistic load modelling

On a given daily load diagram, the load can be taken to be a random variable (L) that follows the same PDF every hour. According to this assumption, the active/reactive loads PDF is below the *normal distribution* [45]:

$$f_L(L)=\frac{1}{\sigma\sqrt{2\pi}}e^{-(L-\mu)^2/2\sigma^2} \quad (34)$$

Where σ is the SD of L and μ is the mean value displayed as the constant load level on the daily load diagram (DLD). To get the load value, the normal CDF (34) and its inverse (36) were utilised.

$$F_L(L)=\frac{1}{2}\left[1+erf\left(\frac{(L-\mu)}{\sqrt{2\sigma}}\right)\right] \quad (35)$$

$$L=\mu+\sqrt{2}.\sigma.erf^{-1}(2r-1) \quad (36)$$

erf and erf^{-1} are defined in (33).

III. Wind Driven Optimization

III.1. Theoretical background and motivation of WDO

Wind blows in the atmosphere to try and balance out variations in air pressure [46]. More precisely, from high pressure to low pressure, the air is employed to move at a speed proportionate to the pressure gradient [49]. WDO is based on Newton's second rule of motion, which is known to produce extremely accurate results when used in the study of atmospheric motion [50–51].

$$\rho\vec{\omega}=\sum\vec{F}_i \quad (37)$$

ρ is the air density for an infinitesimal air parcel, $\vec{F}_i$ is the sum of all forces acting on the air parcel, and $\vec{\omega}$ is the acceleration vector. The ideal gas law is the equation that connects air pressure to temperature and density.

$$P=\rho RT \quad (38)$$

P stands for pressure, *R* for the universal gas constant, and *T* for temperature. In equation (37), the wind is influenced by four primary factors which can either direct its motion or divert it from its intended course [46]. Although the friction force $\vec{F}_F$ just acts to prevent such motion, the pressure gradient force $\vec{F}_{PG}$ is the most noticeable factor driving air movement. When transferred to N-dimensional space, the gravitational force FFG behaves as a vertical force in a three-dimensional atmosphere. The wind is deflected from one dimension to another by the Coriolis force (FC), which is brought about by the earth's rotation [46], [49].

It is represented in WDO as a motion in one dimension influencing a velocity in another. The physical force equation due to pressure gradient can be represented as [51] by assuming that air has a finite volume (δV)

$$\vec{F}_{PG}=-\vec{\nabla}P\,\delta V \quad (39)$$

The air parcel motion that the F_{PG} initiated is opposed by the frictional force, which is simply stated as

$$\vec{F}_F=-\rho\alpha\vec{v} \quad (40)$$

The air parcel experiences a vertical motion that is described as gravity pulling it towards the centre of the earth.

$$\vec{F}_G=\rho\delta V\vec{g} \quad (41)$$

Air parcel motion is deflected by the Coriolis force, so named because of the way the planet rotates [46]. This force will act in a way that affects a direction's velocity without affecting its own. It could be expressed as

$$\vec{F}_C = -2\Omega\vec{v} \tag{42}$$

The pressure gradient is denoted by $\nabla\vec{P}$; the frictional coefficient is represented by α, the wind velocity vector is denoted by $\vec{v}$; δV stands for an infinitesimal air volume, the gravitational acceleration is denoted by $\vec{g}$, and the earth's rotation is Ω. Consequently, the sum of adding $\vec{F}_{PG}$, $\vec{F}_F$, $\vec{F}_G$, and $\vec{F}_C$ to the total force given in (37) can be expressed as

$$\rho\frac{\Delta\vec{v}}{\Delta t} = \rho\vec{v}\Delta t = \vec{F}_{PG} + \vec{F}_F + \vec{F}_G + \vec{F}_C = \rho\delta V\vec{g} + \left(-\nabla\vec{P}\delta V\right) + \left(-\rho\alpha\vec{v}\right) + \left(-2\Omega\vec{v}\right) \tag{43}$$

To keep things simple, we'll assume that the acceleration is equal to $\Delta u/\Delta t$, $\Delta t = 1$, and $\delta V = 1$ for each unit step. Thus, the following is a new formulation of Newton's second law:

$$\rho\Delta\vec{v} = \rho\vec{v}\Delta t = \rho\vec{g} + \left(-\nabla\vec{P}\right) + \left(-\rho\alpha\vec{v}\right) + \left(-2\Omega\vec{v}\right) \tag{44}$$

When ideal gas in (44) represents the equation that combines air pressure and air density. As a result, by altering (44) in accordance with (39) and dividing by $(RT/P_{(k)})$, the change in velocity in (44) can be obtained.

$$\vec{v}_{(k+1)} = \left(1-\alpha-\frac{2\Omega RT}{P_{(k)}}\right)\vec{v}_{(k)} + \vec{g} + \left(-\nabla\vec{P}\frac{RT}{P_{(k)}}\right) \tag{45}$$

The force that pulls an air parcel from its present location towards the earth's centre is known as gravitational force. We may therefore write $g = |g|(0 - x(k))$ [52]-[53] for the vector g. The force that tries to shift an air parcel from its present location into an ideal pressure is known as the pressure gradient. The expression for it is $-\nabla P = |P_{(opt)} - P_{(k)}|(x_{(opt)} - x_{(k)})$. In the final term of (45), all of the coefficients are gathered into a single term known as $c = -2|\Omega|RT$. You can change equation (45) to become as in (46).

$$\vec{v}_{(k+1)} = \left((1-\alpha)\vec{v}_{(k)}\right) + \left(-\vec{g}(x_{(k)})\right) + \frac{RT}{P_{(k)}}|P_{(opt)} - P_{(k)}|(x_{(opt)} - x_{(k)}) + \frac{c\,\vec{v}^{otherd}_{(k)}}{P_{(k)}} \tag{46}$$

Based on the fundamental equation (39) of the ideal gas law, ρ can be expressed in terms of pressure, and for simplicity, a unity time step ($\delta V = 1$) can be taken [49]. With some simplifications, the velocity vector, v, of the WDO method is

$$\vec{v}_{(k+1)} = (1-\alpha)\vec{v}_{(k)} - \vec{g}(x_{(k)}) + \left(\left|\frac{P_{(opt)}}{P_{(k)}} - 1\right|RT(x_{(opt)} - x_{(k)})\right) - \frac{c\,\vec{v}^{otherd}_{(k)}}{P_{(k)}} \tag{47}$$

For the next iteration of (47), the updated velocity, v(k+1), is dependent upon the following: current iteration velocity (v(k)), current air parcel position in search space (x(k)), distance from the highest pressure point discovered (x(opt)), maximum pressure (P(opt)), pressure at the current location (P(k)), temperature (T), gravitational acceleration (g), and constants R, α, and c. Following (46), which updates the parcel velocity, (48) can update the air parcel position [49].

$$\vec{x}_{(k+1)} = \vec{x}_{(k)} + \vec{v}_{(k+1)}\Delta t \tag{48}$$

According to (48), $\vec{x}_{(k)}$ indicates that the air parcel would continue to travel along its original route notwithstanding some resistance brought on by friction. $\vec{v}_{(k+1)}$ is an attracting force that exerts pressure on the coordinate system's centre. In actuality, $x_{(k+1)}$ deflects forces and follows the Coriolis force. In any dimension, if the velocity magnitude exceeds the specialised maximum, the velocity in that dimension is constrained, as per (49)

$$v^* = \begin{cases} v_{\max} & if \quad v_{(k+1)} > v_{\max} \\ -v_{\max} & if \quad v_{(k+1)} < -v_{\max} \end{cases} \tag{49}$$

III.2. Application of WDO to optimal energy management

The position of each of the numerous air parcels that make up the entire solution set is represented by the control variables of the EOM. The location of the ith air parcel in a system with N air parcels is determined by (5). The following steps can be used to summarise the process of applying the WDO algorithm to solve the optimal EOM problem:
Step 1: Specify the data for the DG units, storage units, loads, and MG system settings.
Step 2: Identify the objective function (1), the penalty factor (13), the dependent variable (4), and its lower and upper limitats (8); identify the control variables (5) and their lower and upper limits (7).
Step 3: Set the iteration counter to zero, initialise the WDO parameters, and randomly initialise the position and velocity vectors. Air parcel populations are dispersed at random speeds throughout the search space. The starting air parcels are chosen at random from the control variables minimum and maximum values. Equations (1) and (11) must be used to assess each air parcel selected in the preceding step's position and velocity.
Step 4: Determine the active power from (to) the utility (11) and verify the constraint (8) for each air parcel in the current population.
Step 5: Determine the fitness (1) and (13) for every air parcel.
Step 6: Update the iteration counter t = t + 1.
Step 7: Using (46) and (47), respectively, update each air parcel's velocity and verify the limits.
Step 8: Update each air parcel's position (48).
Step 9: Continue from steps 4–8 until the t_{max} is reached, which is the stop criterion.
Step 10: Stop and return the best solution.

IV. Results and discussion

As seen in Fig. 1, the MG is a standard LV grid-connected. The nickel metal hydride (NiMH-Battery) storage device, MT, FC, WT, and PV DG sources make up the MG. All DG sources are expected to generate active power at unity power factor. Additionally, the utility and MG have a power-exchange link that allows them to trade energy throughout the day in accordance with choices made by the MG central controller (MGCC).

A typical day's load demand inside the MG consists of one feeder that serves a small workshop and is mostly residential, one feeder that serves an industrial region, and one feeder that serves light commercial clients. This adds up to a total energy demand of 1695 kWh for the MG. The bid coefficients and the lowest and maximum generations for the DG units in the MG are shown in Table 1. Table 2 provides the hourly predicted load demands, market energy prices, the WT and the PV output powers. The system data are taken from [37], [45].

The deterministic OEM problem of MG is solved optimally for the following three scenarios using the suggested WDO-based approach as follows:

Table 1. Power limits and coefficients of bid functions of the installed DG units.

N° bus	Type	$P_{DG}^{\min}$ (KW)	$P_{DG}^{\max}$ (KW)	Costs coefficient		
				a	*b*	*c*
1	*MT*	6	30	0	0.457	0
2	*FC*	3	30	0	0.294	0
3	*PV*	0	25	0	2.584	0

4	WT	0	15	0	1.073	0
5	battery	-30	30	0	0.38	0
6	Utility	-30	30	-	-	-

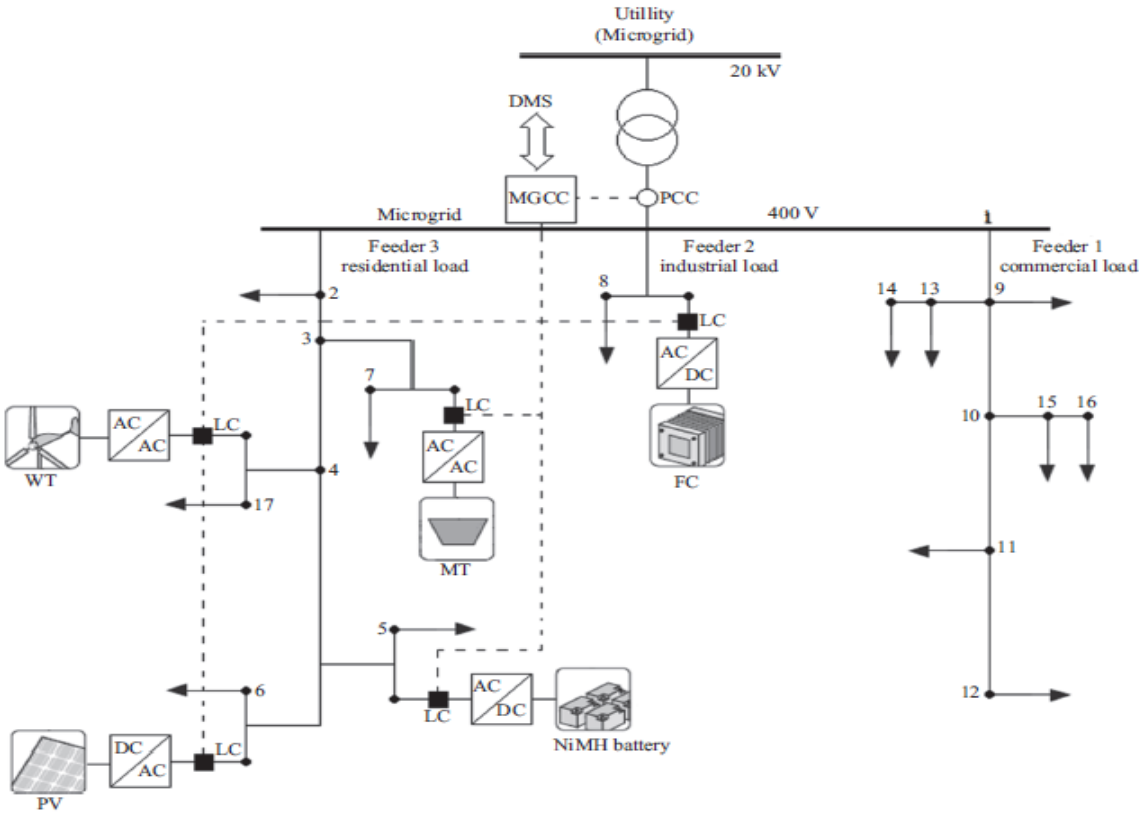

Figure 1. Microgrid test system.

Table 2. Forecast values of the load demand, market price, output powers of WT and PV.

Time [h]	Load [MW]	Market prices ($/kWh)	WT and PV output powers	
			WT	PV
1	480	0.23	2.8	0
2	480	0.19	2.8	0
3	600	0.14	2.8	0
4	600	0.12	2.8	0
5	720	0.12	5.6	0
6	720	0.2	5.6	0
7	840	0.23	5.6	0
8	840	0.38	5.6	0.2
9	960	1.5	5.6	3.75
10	960	4	5.6	7.525
11	1080	4	11.2	10.45
12	1080	4	11.2	11.95
13	1200	1.5	11.2	23.9
14	1200	4	11.2	21.05
15	1080	2	11.2	7.875
16	840	1.95	5.6	4.225
17	840	0.6	5.6	0.55
18	960	0.41	5.6	0
19	1080	0.35	11.2	0
20	1080	0.43	11.2	0
21	960	1.17	5.6	0

22	840	0.54	5.6	0
23	720	0.3	5.6	0
24	600	0.26	2.8	0

Case 1: The WT and PV sources are taken to correspond to their maximum powers accessible for each hour of the day. Conversely, the remaining DG sources such as the utility, battery, MT and FC can function within their power limits as long as they meet the required limitations. Inside the MG, all DGs with comparable features produce electricity. Any excess energy or additional demand inside the grid is traded with the utility from the point of common coupling (PCC) as shown in Fig. 1.

Case 2: All DGs, including the utility, WT and PV are expected to be able to function within their power limitations while meeting the necessary requirements in this scenario.

Case 3: The utility is assumed to act as an unconstrained unit in this scenario, exchanging energy with the MG without any restrictions, while the remaining DGs behave as in Case 2.

The forecasting output powers of PV and WT are displayed in Fig. 2(a) and Fig. 2(b), respectively. Both figures are scaled over a 24-hour period. Figures 3(a) and Fig. 3(b), respectively display the daily load diagram and projected utility price, which are used to test the WDO.

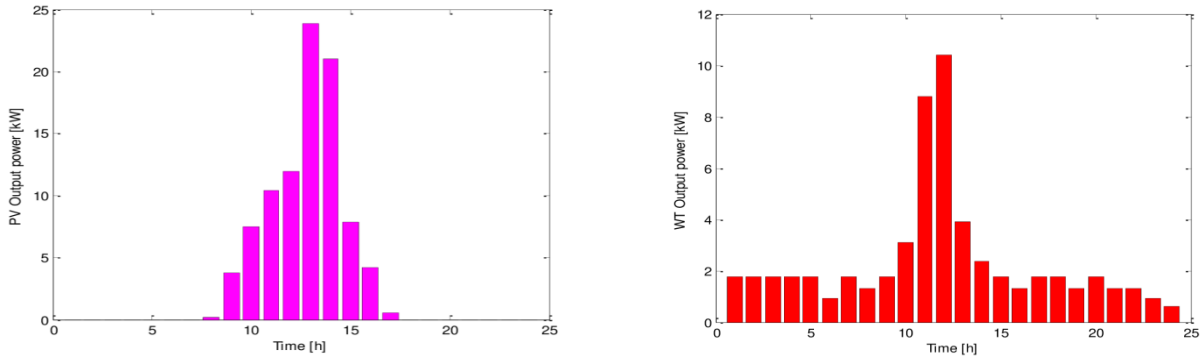

(a) (b)

Figure 2. Forecasted power, (a) PV and (b) WT.

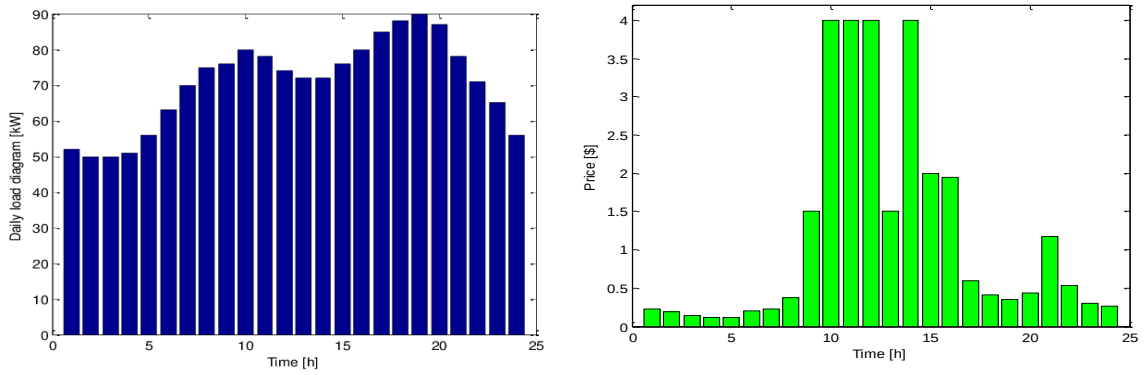

(a) (b)

Figure 3. (a) Forecasted market prices and (b) Daily load diagram.

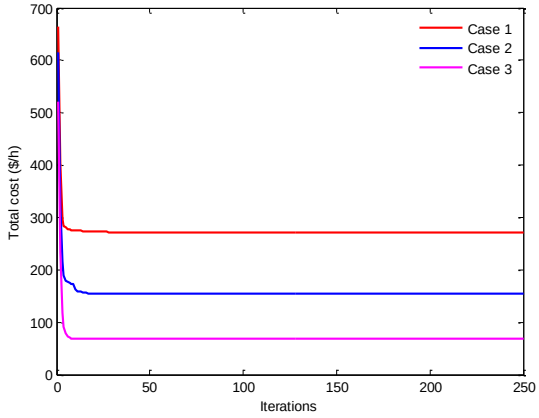

Figure 4. Convergence characteristics of *WDO* method.

The paper uses the following WDO parameters: α=0.4 for the friction coefficient, g=0.2 for the gravitational constant, v=3 for the wind velocity vector, the coefficient RT=3, and c=0.4 for the Coriolis constant. The population size N and maximum iteration number (t_{max}) are fixed at 40 and 250 for each case study, respectively.

In this study, the cost minimization is carried out for a full day, or 24 hours. Figures 4–6, respectively, show the best outcomes for all cases (1, 2, and 3) that were achieved using the WDO approach. Additionally, figure 4 displays the WDO fast convergence characteristics for the top three outcomes of three cases. The optimal output power from the generation sources (FC, MT, PV, and WT) to meet the load demands during the day is displayed in Fig. 5. It is evident from examining these data that every equality and inequality requirement is met.

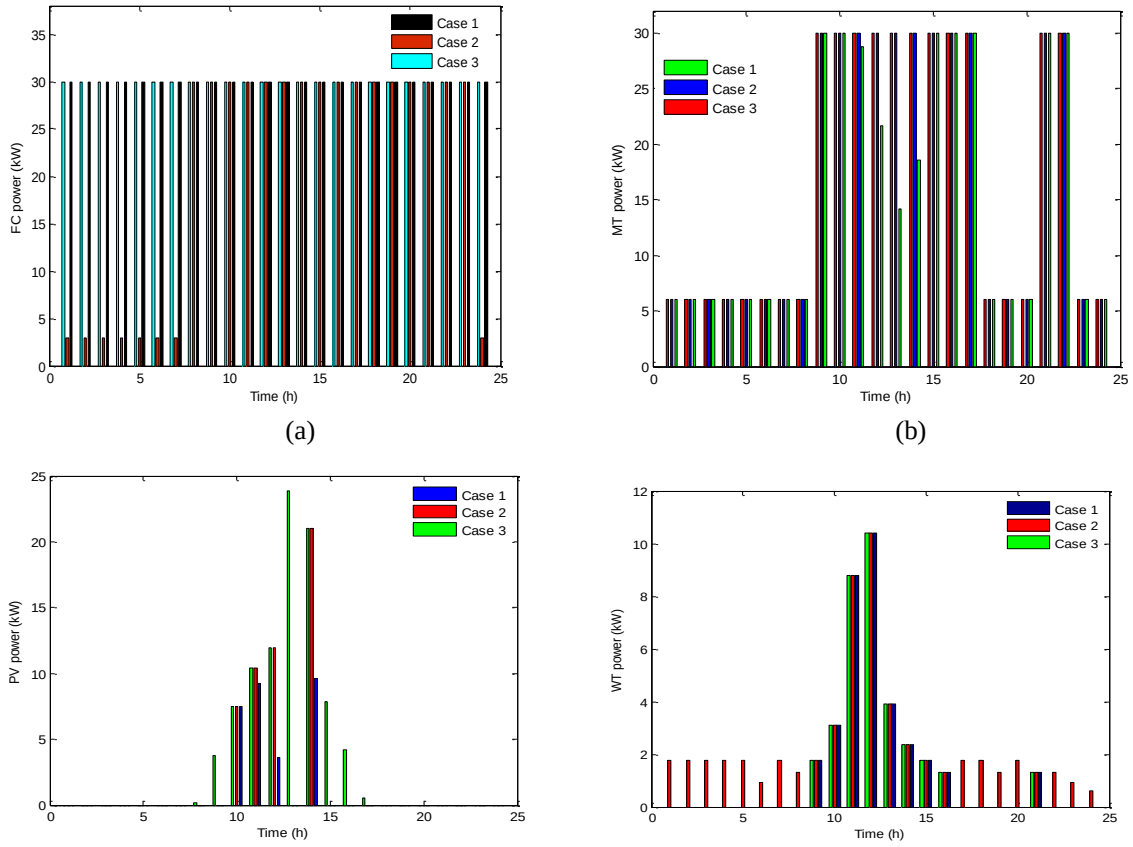

.

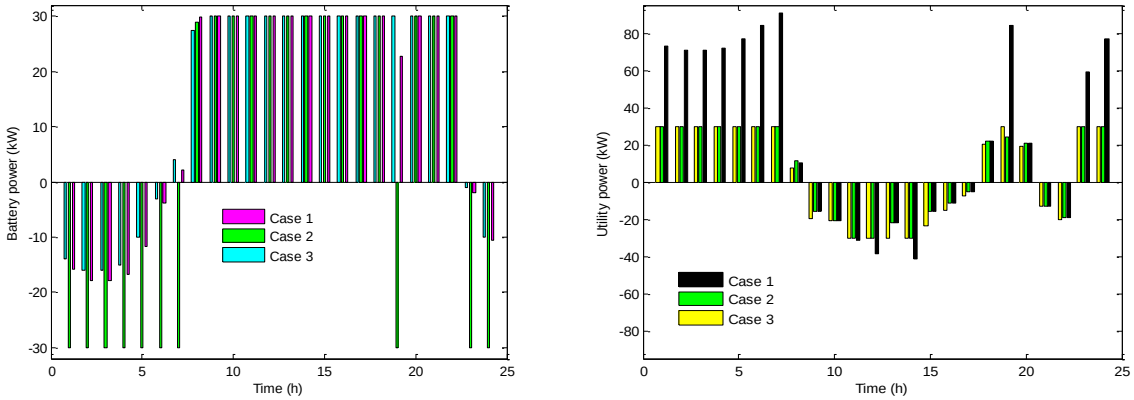

. (e) (f)

Figure 5. Output power, (a) powers provided by the FC and (b) powers provided by the MT, (c) powers provided by the PV, (d) powers provided by the WT, (e) battery powers and (f) utility powers.

Since the market rates are higher between the hours of 9-17 and 21- 22 of the day, MT production capacity is expanded and excess energy from MG is exported to the utility. Regarding battery charging, it happens between the hours of 1-6 h and 23-24 h, when market prices are at their lowest. In this scenario, 271.1968 [$/h] is the best operation cost that was found.

According to case 2, there has been a considerable decrease in MG operating costs when compared to case 1, with a reduction in related costs of 42.77%. The best operation cost in this instance is 155.1933 [$/h]. This is due to WT and PV far lower participation, despite their significantly larger bids than those of the other DGs.

Like in instance 1, the MT output power reaches its maximum value during times of high market prices and its smallest value during times of low market prices. In contrast, the FC output power remains at its maximum value all day long. Low market rate periods are when battery charging occurs, and during these times, energy is transferred from the utility to the MG.

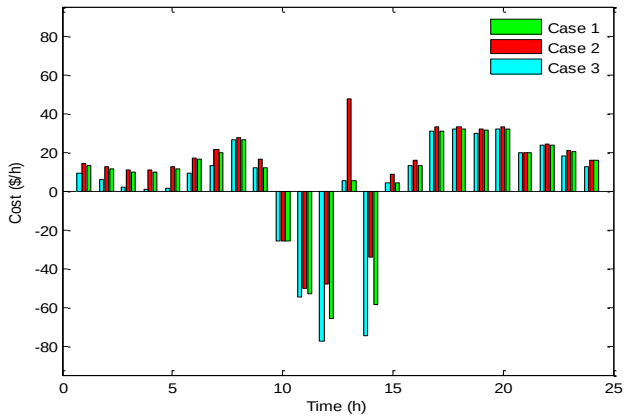

Figure 6. Cost for the 3 cases of simulation.

According to case 3, the optimal operation cost was achieved at 67.7162 [$/h], with MG operating costs being reduced by 75.03%, and 56.36% respectively, in comparison to examples 1 and 2.

Assume case 3, where energy purchases in significant amounts of MG occur during peak times, and lead in supplying the load inside the MG during the periods 1 to 8 hours taken by the utility, in 19 hours and 23 to 24 hours, when the market price is low. Figure 6 displays the current state of each DG and utility grid, respectively. It is evident that 118.8942 [kWh] is the ideal size of ESS in this situation.

From an economic perspective, the PV and WT begin to generate when there is a shortfall of power generation within the MG or when more electricity needs to be exported to the utility. Similar to this, additional DGs like FC, MT, and battery are used to economically alter generation based on load levels at each hour of the day.

A comparison of the obtained and literature results is presented in Table 3. The simulation findings in this research demonstrate how well the WDO approach works to address the OEM of MG. Therefore, the above results demonstrate the capability of the WDO algorithm to produce of higher quality solutions.

Table 3. Comparison of obtained and literature results.

Case	Method	Reference	Best solution
Case 1	WDO	**Proposed**	**271.1968**
	PSO	[45]	269.7599
		[37]	277.3237
	CPSO	[37]	275.0455
	GA	[37]	277.7444
	GSA	[37]	275.5369
Case 2	WDO	**Proposed**	**155.1933**
	PSO	[45]	155.01333
		[37]	162.0083
	CPSO	[37]	161.0580
	GA	[37]	162.9469
Case 3	WDO	**Proposed**	**67.7162**
	PSO	[45]	68.1762
		[37]	90.7629
	CPSO	[37]	90.5545
	GA	[37]	91.3293

V. Conclusion

In this paper, an effective approaches based on *WDO* method is successfully applied to solve the *OEM* problems of a *MG*. The output power of PV and WT, the load demand, and the market price are all modelled using *Weibull and normal distributions*. The suggested method has been investigated and tested on an MG that is connected to various DG units via an ESS. The outcomes of the simulation demonstrate how well the suggested method for resolving the OEM worked in various operational settings (case studies). Furthermore, the outcomes obtained using WDO are either on par with or superior to those obtained by other techniques that have been documented in the literature. The suggested approach produces extremely efficient results while handling global optimisation issues in terms of excellence, computing effort, convergence speed, performance, and quality of solutions. The comparison findings support the suggested approach's superiority over a few different approaches to solve the OEM problem.

References

[1] Zia, M. F. et al., "Energy management system for an islanded microgrid with convex relaxation", *IEEE Transactions on Industry Applications*, vol. 55, No.6, pp. 7175–7185, 2019.

[2] H. Wu, H. Li, and X. Gu, "Optimal energy management for microgrids considering uncertainties in renewable energy generation and load demand", *Processes*, vol. 8, No. 9, p. 1086, 2020.

[3] Benachour Souheyla, Bendjeghaba Omar, "Golden Jackal Algorithm for Optimal Size and Location of Distributed Generation in Unbalanced Distribution Networks", *Algerian Journal of Renewable Energy and Sustainable Development*, vol. 5, No. 1 pp. 28–39, 2023.

[4] F. A. Mohamed, and H. N. Koivo, "Online management genetic algorithms of microgrid for residential application ", *Energy Conversion and Management*, vol. 64, pp. 562–568, 2012.

[5] C. Chen, et al., "Smart energy management system for optimal microgrid economic operation", *IET renewable power generation*, vol. 5, No. 3, pp. 258–267, 2011.

[6] J. Radosavljevic´, M. Jevtic´, and D. Klimenta, "Energy and Operation Management of a microgrid using particle swarm Optimization", *Engineering Optimization*, vol. 48, No. 5, pp. 811–830, 2016.

[7] J. A. P. Lopes, C. L. Moreira, and A. G. Madureira, "Defining control strategies for microgrids islanded operation", *IEEE Transactions on power systems*, vol. 21 No. 2, pp. 916–924, 2006.

[8] N. D. Hatziargyriou, et al. "Quantification of economic, environmental and operational benefits due to significant penetration of microgrids in a typical LV and MV Greek network", *European Transaction on Electrical Powe*r, vol. 21, No. 2, pp. 1217–1237, 2011.

[9] A. G. Tsikalakis, N. D. Hatziargyriou, "Centralized control for optimizing microgrids operation", *IEEE Transactions on Energy Conversion*, vol. 23, No. 1, pp. 241–248, 2008.

[10] T. S. Ustun, C. Ozansoy, and A. Zayegh, "Recent developments in microgrids and example cases around the world—a review ", *Renewable and Sustainable Energy Reviews*, vol. 15, pp. 4030–4041, 2011.

[11] J. Radosavljević, et al., "Optimal power flow for distribution networks with distributed generation", *Serbian Journal of Electrical Engineering*, vol. 12, No. 2, pp. 145–170, 2015.

[12] A. Arabali, M. Ghofrani, M. Etazadi-Amoli, S. Fadali, and Y. Baghzouz, "Genetic-algorithm-based optimization approach for energy management", *IEEE Transactions on Power Delivery*, vol. 28, No. 1, pp. 162–170, 2013.

[13] E. Kuznetsova, C. Ruiz, Y. F. Li, and E. Zio, "Analysis of robust optimization for decentralized microgrid energy management under uncertainty", *International Journal of Electrical Power & Energy Systems*, vol. 64, pp. 815–832, 2015.

[14] K. F. Fong, V. I. Hanby, T. T. Chow, "HVAC system optimization for energy management by evolutionary programming", *Energy and Buildings*, vol. 18, No.3 pp. 220-231, 2006.

[15] S. Mandal, and K. K. Mandal, "Optimal energy management of microgrids under environmental constraints using chaos enhanced differential evolution", *Renewable Energy Focus*, vol. 34, pp. 129-141, 2020.

[16] N. Nikmehr, and S. N. Ravadanegh, "Optimal operation of distributed generations in micro-grids under uncertainties in load and renewable power generation using heuristic algorithm", *IET Renewable Power Generation*, vol. 9, No. 8, pp. 982–890, 2015.

[17] M. A. Kamarposhti, I. Colak , K. Eguchi, "Optimal energy management of distributed generation in micro-grids using artificial bee colony algorithm", *Mathematical Biosciences and Engineering*, vol. 18, No. 6, pp. 7402-7418, 2021.

[18] A. Esmat, et al., "A novel Energy Management System using Ant Colony Optimization for micro-grids", *3rd International Conference on Electric Power and Energy Conversion Systems (EPECS)*, 2013.

[19] P. Li, W. Xu, Z. Zhou, and R. Li, "Optimized operation of microgrid based on gravitational search algorithm", *Proceedings of International Conference on Electrical Machines and Systems*, Busan, Korea, pp. 338–42, 2013.

[20] N. Javaid, et al., "A Hybrid Genetic Wind Driven Heuristic Optimization Algorithm for Demand Side Management in Smart Grid", *Energies*, vol. 10, No. 3, pp. 319-346, 2017.

[21] M. Y. Alsmadi et al., "Optimal configuration and energy management scheme of an isolated micro-grid using Cuckoo search optimization algorithm", *Journal of the Franklin Institute*, vol. 356, pp. 4191-4214, 2019.

[22] S. Kutaiba, et al., "Grey Wolf Optimization-Based Optimum Energy-Management and Battery-Sizing Method for Grid-Connected Microgrids", *Energies*, vol. 11, No. 4, pp. 847-864, 2022.

[23] M. A. Ríos, and A. M. V. Rodríguez, "Multi-objective Firefly Algorithm for Energy Optimization in Grid Environments", *International Conference on Swarm Intelligence*, vol. 7461, pp. 350–351.

[24] W. A. Hasan, I. A. Abed, D. K. Shary, "Energy Management Optimization of Generators Using Modified Firefly Algorithm", *2nd International Multi-Disciplinary Conference Theme*: Integrated Sciences and Technologies, IMDC-IST, 7-9, Sakarya, Turkey, September 2021.

[25] B. Hernández-Ocaña et al., "Bacterial Foraging-Based Algorithm for Optimizing the Power Generation of an Isolated Microgrid", *Applied Sciences*, vol. 9, No. 6, pp.1261, 2019.

[26] B. Bentouati et al., "An enhanced moth-swarm algorithm for efficient energy management based multi dimensions OPF problem", *Journal of Ambient Intelligence and Humanized Computing*, vol. 12, No. 1, pp. 1-21, 2020.

[27] S. Debata, C. K. Samanta, and S. P. Panigrahi, "Efficient energy management strategies for hybrid electric vehicles using shuffled frog-leaping algorithm", *International Journal of Sustainable Engineering*, vol. 8, No. 2, pp. 1-7, 2015.

[28] F. A Mohamed, and H. N. Koivo, "System modelling and online optimal management of microgrid using mesh adaptive direct search", *International Journal of Electrical Power & Energy Systems*, vol. 32, No. 5, pp. 398–407, 2010.
[29] M. I. Normazlina, T. C. Wei, A. H. M. Yatim, "Energy Management for an Islanded Microgrid Based on Harmony Search Algorithm", 41st International Spring Seminar on Electronics Technology (ISSE), pp. 16-20 May 2018.
[30] R. Krishna, and S. Hemamalini, "Optimal Energy Management of Virtual Power Plants with Storage Devices Using Teaching-and-Learning-Based Optimization Algorithm", *International Transactions on Electrical Energy Systems*, vol. 2022, pp. 1-17, 2022.
[31] I. Hussain, et al., "Smart Energy Management System for University Campus using Sine-Cosine Optimization Algorithm", International Virtual Conference on Power Engineering Computing and Control: Developments in Electric Vehicles and Energy Sector for Sustainable Future (PECCON), 05-06 May 2022.
[32] A. Rabiee, M. Sadeghi, J. Agha, "Modified imperialist competitive algorithm for environmental constrained energy management of microgrids", *Journal of Cleaner Production*, vol. 20, pp. 273-292, 2018.
[33] J. D. Tan, et al., "An Electromagnetism-like Mechanism Algorithm Approach for Photovoltaic System Optimization", *Indonesian Journal of Electrical Engineering and Computer Science*, vol. 12, No. 1, pp. 333-340, 2018.
[34] J. Radosavljević, "Metaheuristic Optimization in Power Engineering", The Institution of Engineering and Technology, *Michael Faraday House*, Six Hills Way, Stevenage, Herts, SG1 2AY, United Kingdom, 2018.
[35] Y. Zhang, N. Gatsis, and G. B. Giannakis, "Robust energy management for microgrids with high-penetration renewable", *IEEE Transactions on Sustainable Energy*, vol. 4, No. 4, pp. 944–953, 2013.
[36] Wu H., Liu X., Ding M. "Dynamic economic dispatch of a microgrid: Mathematical Models and Solution Algorithm", *International Journal of Electrical Power and Energy Systems*, vol. 63, pp. 336–346, 2014.
[37] A. A. Moghaddam, A. Seifi, T. Niknam, and M. R. A. Pahlavani, " Multi-objective operation management of a renewable MG (micro-grid) with back-up micro-turbine/fuel cell/battery hybrid power source", *Energy*, vol. 36, pp. 6490–6507, 2011.
[38] A. M Azmy, I. Erlich, "Online optimal management of PEM fuel cells using neural networks", *IEEE Transactions on Power Delivery*, vol. 20, No. 2, pp 1051–1058, 2005.
[39] S. Campanari, and E. Macchi, "Technical and tariff scenarios effect on microturbine trigenerative applications", *Journal of Engineering for Gas Turbines and Power*, vol. 126, pp. 581–589, 2004.
[40] F. Barbir, and T. Gomez, "Efficiency and economics of proton exchange membrane (PEM) fuel cells", *International Journal of Hydrogen Energy*, vol. 22, No. 10/11, pp. 1027–1037, 1997.
[41] D. Villanueva, J. L. Pazos, and A. Feijo, "Probabilistic load flow including wind power generation", *IEEE Transactions on Power Systems*, vol. 26, No. 3, pp. 1659–1667, 2011.
[42] Nasreddine Belbachir, and Mohamed Zellagui, "Multi-Objective Optimal Design of Solar and Wind Hybrid Renewable Energy Systems Considering Daily Uncertainties", *Algerian Journal of Renewable Energy and Sustainable Development*, vol. 4, No.1, pp. 1-15, 2022.
[43] G. N. Tiwari, and S. Dubey, "Fundamentals of photovoltaic modules and their applications", *Energy Series Cambridge*, p. 423. 2010.
[44] M. N. Amroun, K. Salim, M. A. Ghezal, A. H. Kacha, M. Khadraoui, "Models for evaluating the maximum power produced by a Photovoltaic generator", *Algerian Journal of Renewable Energy and Sustainable Development*, vol. 3, No. 2, pp. 132–140, 2021.
[45] J. Radosavljević, M. Jevtić and D. Klimenta, "Energy and operation management of a microgrid using particle swarm optimization", *Engineering Optimization*, vol. 48, No. 5, pp. 811-830, 2015.
[46] Z. Bayraktar, M. Komurcu, and D. H. Werner, "Wind Driven Optimization (WDO): A Novel Nature-Inspired Optimization Algorithm and its Application to Electromagnetics", *IEEE Antennas and Propagation Society International Symposium*, pp. 1-4, 2010.
[47] Z. Bayraktar, et al., "Stub-loaded Inverted-F Antenna Synthesis via Wind Driven Optimization", *IEEE International Symposium on Antennas and Propagation (APSURSI)*, pp. 2920-2923, 2011.

[48] Z. Bayraktar, M. Komurcu, "The Wind Driven Optimization Technique and its Application in Electromagnetics", *IEEE Transactions on Antennas and Propagation*, IEEE, 2013.
[49] P. Lakshminarayana, and S. Ravindra, "Wind Driven Optimization Technique: Optimal power flow problem", *International Journal of Applied Engineering Research*, vol. 12, No. 1, pp. 308-313, 2017.
[50] B. Zongfan, Z. Yongquan, L. Liangliang, and M. Mingzhi, "A Hybrid Global Optimization Algorithm Based on Wind Driven Optimization and Differential Evolution", *Hindawi Publishing Corporation Mathematical Problems in Engineering*, vol. 2015, pp. 1-20, 2015.
[51] U. Ashwini, M. E. A. Ravi, and J. D. Sathyara, "Wind Drive Optimization Based Economic Dispatch for the Effective Micro Grid Utilization", *International Journal of Advanced Research in Basic Engineering Sciences and Technology*, vol. 3, No. 24, pp. 760-766, 2017.
[52] O. Abdalla, H. Rezk, and E. A. Ahmed, "Wind Driven Optimization Algorithm based Global MPPT for PV System Under non-uniform Solar Irradiance", *International Solar Energy Society*, Published by Elsevier Ltd, vol. 180, pp. 429-444, 2019.
[53] S. Kaur, and A. Kumar, "Application of Wind Driven Optimization Algorithm for Clustering in WSN to Achieve Energy Efficiency", *International Journal for Scientific Research and Development*, vol. 3, No. 6, 2015.
[54] A. Recioui, M. Benabid, and N. Djilani, "Rectangular Antenna Array Optimization usig Wind Driven Optimization", *Algerian Journal of Signals and Systems*, vol. 1, No. 2, pp. 109-120, 2016.
[55] H. H. Alhelou, M. E. H. Golshan, and M. H. Fini, "Wind Driven Optimization Algorithm Application to Load Frequency Control in Interconnected Power Systems Considering GRC and GDB Nonlinearities", *Electric Power Components and Systems*, vol. 46, No. 11-12, pp. 1223-1238, 2018.